THE JOURNAL OF BIOLOGICAL CHEMISTRY
Vol. 277, No. 39, Issue of September 27, pp. 36296–36303, 2002

Printed in U.S.A.

Differential Localization of the Vacuolar H^+ Pump with *G* Subunit Isoforms (*G*1 and *G*2) in Mouse Neurons*

Received for publication, January 18, 2002, and in revised form, July 15, 2002
Published, JBC Papers in Press, July 19, 2002, DOI 10.1074/jbc.M200586200

Yoshiko Murata‡§¶, Ge-Hong Sun-Wada‡§¶, Takao Yoshimizu‡§, Akitsugu Yamamoto§‖, Yoh Wada‡§, and Masamitsu Futai‡§**

From the ‡Division of Biological Sciences, Institute of Scientific and Industrial Research, Osaka University and the §Core Research for Evolutional Science and Technology (CREST) of the Japan Science and Technology Corporation, Osaka 567-0047, Japan and the ‖Department of Physiology, Kansai Medical University, Moriguchi, Osaka 570-8506, Japan

Vacuolar H^+-ATPases (V-ATPases), a family of multimeric proton pumps, are involved in a wide variety of physiological processes. We have identified two mouse genes, *Atp6g1* and *Atp6g2*, encoding the *G*1 and *G*2 isoforms of the V-ATPase *G* subunit, respectively. *G*1 was distributed ubiquitously in the tissues examined, whereas *G*2 was specifically distributed in central nervous system neurons. *G*1 was expressed at an early embryonic stage, whereas *G*2 transcription was significantly induced at 10.5 days postcoitus (embryonic day 10.5, *i.e.* 2 days before axon outgrowth). Both *G*1 and *G*2 were strongly expressed in cortical and hippocampal neurons, cerebellar granule cells, and Purkinje cells. Immunohistochemistry with isoform-specific antibodies revealed that *G*2 was localized in cell bodies, dendrites, and axons. In addition, electron microscopy and subcellular fractionation indicated that *G*2 was localized in synaptic vesicles, whereas *G*1 was not detectable. *G*1 and *G*2 exhibit 62% identity, and both isoforms were immunoprecipitated with the *c* and *A* subunits of V-ATPase. *G*2 could complement the yeast deletion mutant Δ*vma10*, which lacks the *G* subunit. The V-ATPases containing the *G*1 and *G*2 isoforms, respectively, showed similar $K_{m(ATP)}$ values and maximal velocity. These results indicate that *G*1 and *G*2 are *bona fide* subunits of V-ATPases and that the enzyme with the *G*2 isoform is involved in synaptic vesicle acidification.

The vacuolar H^+-ATPases (V-ATPases),[1] which are ATP-dependent proton pumps, are ubiquitous enzymes that translocate H^+ across the membranes of endomembrane organelles, including vacuoles, lysosomes, endosomes, the Golgi apparatus, chromaffin granules, and coated vesicles (1–3). The same type of enzyme is also found in the plasma membranes of specialized cells such as osteoclasts and renal epithelial cells (4, 5). Thus, V-ATPases could be localized in different organelles and membranes, leading to their specific functions.

In neurons, the pH gradient (pH ~5.2 inside) (6, 7) and membrane potential generated by V-ATPase drive the neurotransmitter accumulation in synaptic vesicles (8, 9). The neurotransmitters are released from nerve terminals upon regulated exocytosis of the vesicles (8–11). V-ATPase activity is also essential for intracellular membrane trafficking, processing or degradation of proteins, and receptor-mediated endocytosis in other organelles of neuronal cells.

V-ATPases (V_1V_0) have a structure and mechanism similar to those of F-type ATPases (ATP synthases, F_1F_0), and their ATP-dependent conformational changes are transmitted from the membrane extrinsic sector (V_1 or F_1) to the proton pore (V_0 or F_0) through a number of subunits forming a stalk (1–3). Studies on knockout mice lacking the V_0 *c* subunit, encoded by a single gene (12, 13), have indicated that V-ATPases are essential for early development (14, 15).

The diverse functions of V-ATPases may be due to the utilization of a specific subunit isoform(s). Consistent with this notion, multiple subunit isoforms have been found for the largest subunit, *a*, of the V_0 sector in nematode (16), chicken (17), mouse (18–21), cow (22), and man (23). *a*4 is specifically expressed in renal intercalated cells (20, 21, 23), and mutations of it cause renal acidosis (23), whereas other isoforms (*a*1, *a*2, and *a*3) are expressed ubiquitously in the tissues examined (17–19). Isoform *a*3 is a component of osteoclast plasma membrane enzyme (18), and its defect results in osteopetrosis (24). In the case of the mammalian V_1 sector, the expression of *B*1 is strictly limited to kidney and cochlea (25), whereas *B*2 is expressed ubiquitously. We have recently identified two isoforms (*E*1 and *E*2) of the mouse *E* subunit (26). In contrast to the ubiquitously distributed *E*2 subunit, *E*1 is expressed specifically in testis and is required for acrosome acidification. Thus, V-ATPases may have two kinds of isoforms: those expressed in specific cells (*a*4, *B*1, and *E*1) and those that show specific localization after cellular differentiation (*a*3).

The bovine *G* subunit was shown to contain two kinds of isoforms, although the expression pattern and localization of each isoform were not shown (27). In this study, we have characterized two mouse genes, *Atp6g1* and *Atp6g2*, encoding the *G*1 and *G*2 isoforms of the V-ATPase *G* subunit, respectively. *G*2 was found exclusively in central nervous system neurons and exhibits high similarity to *G*1, which is expressed ubiquitously. In addition to the cell bodies and dendrites, we found that V-ATPases of the *G*2 isoform were localized in synaptic vesicles in axons, whereas those of the *G*1 isoform were not detectable. Our results constitute the first evidence that a unique V-ATPase with the *G*2 isoform is involved in the

* This work was supported in part by grants-in-aid from the Ministry of Education, Science, and Culture of Japan and the Hayashi and Naito Foundations. The costs of publication of this article were defrayed in part by the payment of page charges. This article must therefore be hereby marked "*advertisement*" in accordance with 18 U.S.C. Section 1734 solely to indicate this fact.

The nucleotide sequence(s) reported in this paper has been submitted to the GenBank™/EBI Data Bank with accession number(s) AB076406 and AB076405.

¶ Both authors contributed equally to this work.

** To whom correspondence should be addressed: Div. of Biological Sciences, Osaka University, Mihogaoka 8-1, Ibaraki, Osaka 567-0047, Japan. Tel.: 81-6-6879-8480; Fax: 81-6-6875-5724; E-mail: m-futai@sanken.osaka-u.ac.jp.

[1] The abbreviations used are: V-ATPases, vacuolar H^+-ATPases; EST, expressed sequence tag; MAP2, microtubule-associated protein-2.

acidification of synaptic vesicles in central nervous system neurons.

EXPERIMENTAL PROCEDURES

Cloning of cDNAs Coding for Mouse G1 and G2 Isoforms—The GenBank™/EBI Data Bank of expressed sequence tags (ESTs) was searched using the yeast Vma10p sequences (28). The mouse EST clone containing the entire open reading frame for the *G*1 or *G*2 isoform was verified by ABI Prism® BigDye™ terminator cycle sequencing (Applied Biosystems, Inc.).

In Situ Hybridization—Digoxigenin-11-UTP-labeled single-stranded RNA probes were prepared with a digoxin/RNA labeling mixture and the corresponding T3 or T7 RNA polymerase (Roche Molecular Biochemicals) according to the manufacturer's instructions. The 498- and 932-bp fragments derived from the 3′-untranslated regions of *G*1 and *G*2, respectively, were cloned into the pBluescript II vector (Stratagene) and used to prepare probes. *In situ* hybridization was performed using 8-μm cryosections of the brains of ICR mice (~8–10 weeks old) as previously described (29). Sections were hybridized with probes at 45 °C for 16 h and then washed successively. For the reaction with anti-digoxigenin antibodies, slides were washed with buffer A (100 mM Tris-HCl and 150 mM NaCl, pH 7.5). Samples were treated with 0.5% blocking reagent (Roche Molecular Biochemicals) in buffer A and then incubated with alkaline phosphatase-coupled anti-digoxigenin antibodies (Roche Molecular Biochemicals) diluted 1:750 in buffer A for 1 h. The slides were washed with buffer A and then incubated in buffer B (100 mM Tris-HCl and 50 mM $MgCl_2$, pH 9.5). Alkaline phosphatase activity was abolished with Tris/EDTA, and the slides were rinsed in water, counterstained with methyl green, and then mounted with Crystal Mount (Biomeda). Whole-mount *in situ* hybridization was performed as previously described (30).

Complementation of Yeast Δvma10 with G1 or G2—The entire open reading frames for *G*1 and *G*2 were amplified by PCR with HiFi™ polymerase (Roche Molecular Biochemicals) and cloned into the pKT10 or pKT10-N-Myc vector (31). The resulting plasmids, pKT-*G*1 (or pKT-N-Myc-*G*1) and pKT-*G*2 (or pKT-N-Myc-*G*2), were transformed into Δ*vma10* (*MATα* Δ*vma10*::*LEU2 ura3-52 leu2-3,112 his4-519 ade6 pep4-3*). Δ*vma10* was generated following the method described previously (32), and gene disruption was confirmed by Southern analysis. The transformants were streaked onto YPD (yeast/peptone/dextrose) plates buffered to either pH 5.0 or 7.5 (33).

Antibodies against V-ATPase Subunits—Polyclonal antibodies against *G*1 or *G*2 were raised in rabbits by immunization with peptides corresponding to each isoform (*G*1, KETREKMTVLQNYFEQNRDE, positions 75–94; *G*2, QATRRQVQGMQSSQQRNRER, positions 75–94). The antisera were purified on affinity columns with coupled bacterially expressed recombinant proteins. The anti-*A* subunit antiserum was from Wako Bioproducts. The anti-*c* subunit antiserum was kindly provided by Dr. S. Ohkuma (34).

Purification of Synaptic Vesicles from Brain and Lysosomal Membranes from Liver—Synaptic vesicles were prepared from mouse brains at 4 °C as described by Huttner *et al.* (35). Briefly, whole mouse brains were homogenized in buffered sucrose (320 mM sucrose and 4 mM HEPES-NaOH, pH 7.4); the homogenate was centrifuged at 800 × *g* for 10 min; and the supernatant (S1) was centrifuged for 15 min at 9200 × *g*. The resulting supernatant (S2) was centrifuged at 100,000 × *g* for 1 h, yielding S3 and P3 (supernatant and pellet, respectively). The 9200 × *g* pellet (P2) was resuspended in the buffered sucrose and centrifuged at 10,200 × *g* for 15 min. The resulting pellet (P2′) was resuspended in the same buffer and homogenized with 9 volumes of ice-cold water. The mixture was added to 1 M HEPES-NaOH, pH 7.4, to a final concentration of 7.5 mM; incubated on ice for 30 min; and centrifuged at 25,000 × *g* for 20 min, yielding the LP1 pellet and LS1 supernatant fraction. LS1 was further centrifuged at 165,000 × *g* for 2 h, and LP2 was suspended in 40 mM sucrose. LP2 was applied to a continuous sucrose gradient (50–800 mM) and centrifuged at 65,000 × *g* for 5 h. Fractions containing synaptophysin (a synaptic vesicle protein marker) were used as synaptic vesicle fractions.

The lysosomal membranes were prepared using OptiPrep (Nycomed Pharma) as described previously (36). The fractions containing the lysosomal membrane marker LAMP-2 (37) were used for measuring ATPase activity.

Measurement of ATPase Activity—ATPase activity was measured using a coupled spectrophotometric assay (26) with minor modifications. For determining the $K_{m(ATP)}$ and V_{max} for V-ATPase, concanamycin-sensitive ATPase activity was measured over a range of ATP concentrations between 0.05 and 2.0 mM. Synaptic vesicles (8 μg of protein) or lysosomal membranes (30 μg of protein) were incubated in assay buffer (5 mM HEPES-NaOH, pH 7.0, 4 mM KCl, 0.3 M sucrose, 5 mM $MgCl_2$, 1.5 mM phosphoenolpyruvate, 0.2 mM NADH, 20 units/ml pyruvate kinase, and 10 units/ml lactate dehydrogenase) with 0.1% dimethyl sulfoxide or 1 μM concanamycin A (in the same solvent) at 37 °C for 2 min. The assay was started by adding various concentrations of ATP, and the absorbance at 340 nm was continuously monitored using a Hitachi UV-2500 PC spectrophotometer.

Solubilization of V-ATPase and Assay of Immunopurified ATPase Activity—For solubilization of V-ATPase, the brain membrane fraction (5 mg/ml) was incubated at 4 °C for 10 min in 20 mM Tris-HCl, pH 7.0, containing 1 mM EDTA, 2% *n*-octyl β-glucopyranoside, 1 mM dithiothreitol, 10% glycerol, 1 mM phenylmethylsulfonyl fluoride, and complete protease inhibitor mixture (Roche Molecular Biochemicals), and then centrifuged at 100,000 × *g* for 30 min. ATPase activity bound to protein A-Sepharose beads was assayed as follows. Anti-*G*1 or anti-*G*2 IgG antibody (100 μg) was incubated in 20 μl of 25 mM Tris-HCl, pH 7.0, containing 136 mM NaCl, 2.7 mM KCl, and a 25% suspension of protein A beads at room temperature for 2 h. Beads were washed twice and resuspended in the same buffer (original volume). The antibody-bound beads were then incubated with solubilized membranes at 4 °C for 1.5 h, rinsed extensively, and resuspended in 20 μl of the same buffer. The ATPase activities were assayed immediately in buffer containing 50 mM Tris-HCl, pH 7.0, 150 mM KCl, 6 mM $MgCl_2$, and 100 μg/ml phosphatidylglycerol with or without concanamycin A using [γ-^{32}P]ATP (0.1–5 mM) (38). The amount of membrane protein bound to the beads was estimated as described previously (39).

Hippocampal and Cerebellar Primary Cultures—Primary cultures of hippocampal and cerebellar cells were carried out using 18.5-day postcoitus embryonic mouse brains (40). In brief, cells were dissociated by gentle homogenization with a fire-polished Pasteur pipette and then plated onto poly-D-lysine-coated culture slides. They were cultured in Neurobasal™ medium (Invitrogen) containing B-27 supplement (Invitrogen), 500 μM L-glutamine, 25 μM L-glutamic acid, and 25 μM β-mercaptoethanol for the first 4 days and maintained by replacing the medium every 4 days.

Immunohistochemistry and Fluorescence Microscopy—Whole brains were obtained from adult ICR mice, cryosectioned at 12 μm, fixed with 4% paraformaldehyde, and then subjected to immunohistochemistry (20). Hippocampal and cerebellar cells cultured for 14 days were fixed with 4% paraformaldehyde and then washed with 0.1 M glycine in phosphate-buffered saline. After blocking with phosphate-buffered saline containing 0.4% saponin, 2% normal goat serum, and 1% bovine serum albumin, cells were labeled with primary and secondary antibodies. After extensive washing with the same buffer, the cells were mounted onto slides with Vectashield (Vector Labs Inc.) and then visualized using a laser scanning confocal imaging system (LSM510, Carl Zeiss, Inc.). The primary antibodies used were anti-microtubule-associated protein-2 (MAP2) (Sigma), anti-2′,3′-cyclic nucleotide 3′-phosphodiesterase (Sigma), anti-glial fibrillary acidic protein (Transduction Laboratories), and anti-synaptophysin (Progen). The secondary antibodies used were fluorescein isothiocyanate-conjugated goat anti-mouse IgG antibodies and Cy3-conjugated goat anti-rabbit IgG antibodies (both from (Jackson ImmunoResearch Laboratories, Inc.). The cells were counterstained with TOPRO-3 (diluted 1:500; Molecular Probes, Inc.) to identify nuclei.

Cell Fractionation and Immunoprecipitation of V-ATPase—All operations were carried out at 4 °C. Adult mouse tissues were dissected and suspended in ice-cold 10 mM HEPES-NaOH, pH 7.4, containing 0.25 M sucrose, 1 mM EDTA, 1 mM dithiothreitol, 1 mM phenylmethylsulfonyl fluoride, and complete protease inhibitor mixture and then homogenized in a Wheaton homogenizer. The lysates, obtained upon centrifugation at 1000 × *g* for 5 min, were centrifuged at 8000 × *g* for 10 min. The supernatants were further centrifuged at 100,000 × *g* for 60 min. The pellets suspended in phosphate-buffered saline containing 1 mM EDTA and 10% glycerol were used as membrane fractions. Western blotting was carried out as previously described (18). For immunoprecipitation of V-ATPase, the supernatant (solubilized V-ATPase) was incubated with 1 μg of anti-*G*1 or anti-*G*2 antibody or preimmune IgG for 1 h and then with protein A-Sepharose beads for 1 h. After washing the beads six times with the above buffer, the immunoprecipitates were boiled in sample buffer (41) and subjected to Western blotting.

Electron Microscopy—The pre-embedded silver enhancement immunogold method was used (26). After perfusion with 4% paraformaldehyde and 0.2% picric acid in phosphate-buffered saline, the mouse brain was dissected and fixed in the same solution at 4 °C for 2 h. Cryosec-

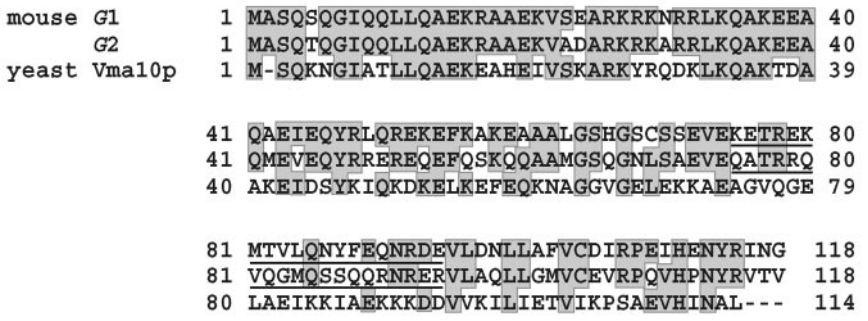

FIG. 1. **Alignment of the amino acid sequences of *G* subunit isoforms.** The sequences of mouse *G* subunit isoforms and yeast Vma10p were aligned to obtain maximal homology. Identical residues are indicated by *gray boxes*, and the regions used for antibody preparation are *underlined*.

tions (6 μm) were reacted with primary antibodies overnight, followed by incubation with colloid gold (1.4-nm diameter)-conjugated secondary antibodies. The gold labeling was intensified using a silver enhancement kit (Nano Probes).

RESULTS

Identification of Mouse G Isoforms—Similarity searches with the yeast Vma10p (*G* subunit) amino acid sequence revealed the presence of related mouse EST clones in the GenBank™/EBI Data Bank and the RIKEN Full-length cDNA Project Database (42). The mouse EST clones fall into two categories, both of which are homologous to Vma10p, indicating the presence of two genes. We have determined the sequences of two EST clones (DDBJ/GenBank™/EBI accession numbers BG175176 and BG296113) and named the proteins encoded by them the *G*1 and *G*2 isoforms, respectively.

Both isoforms comprise 118 amino acid residues and show high homology (76% similarity) to yeast Vma10p (Fig. 1). *G*1 and *G*2 exhibit 62% identity to each other. The amino-terminal regions of *G*1 and *G*2 are highly conserved, whereas their carboxyl-terminal regions are variable (Fig. 1). The mouse genes encoding *G*1 and *G*2 were designated as *Atp6g1* and *Atp6g2*, respectively. They were mapped to chromosomes 4 and 17, respectively, according to the RIKEN Database.[2] The GenBank™/EBI accession numbers for the cDNAs (*Atp6g1* and *Atp6g2*) are AB076406 and AB076405, respectively.

Expression of Isoforms in Developing and Adult Central Nervous System Neurons—The 1.2-kb *G*1 transcript was detected in all tissues examined, whereas the 1.6-kb *G*2 transcript was expressed predominantly in brain (Fig. 2*A*). Consistent with its ubiquitous expression, *G*1 was detected from an early embryonic stage (4.5 days postcoitus). On the other hand, *G*2 was induced at 10.5 days postcoitus and was maintained at all subsequent stages (Fig. 2*B*). 10.5 days postcoitus is the stage when the first motor neurons are established, with the outgrowth of axons starting 2 days later (43).

Upon whole-mount *in situ* hybridization of 10.5-day postcoitus embryos, *G*1 mRNA was detected in all tissues (Fig. 3*A*), whereas *G*2 was exclusively expressed in the central nervous system (Fig. 3*B*, *arrowheads*). Both isoforms were highly expressed in similar regions of the adult brain (Fig. 3*C*). They were strongly expressed in the cerebral cortex; dentate gyrus; the pyramidal neurons in the Ammon's fields of the hippocampus; and Purkinje cells in the cerebellum.

Specific Antibodies for G1 and G2—The antibodies raised against *G*1 or *G*2 using specific peptides (Fig. 1) recognized the corresponding isoform expressed in yeast (Fig. 4*A*). Immunoblotting with anti-*G*2 IgG antibody revealed an 18-kDa protein only in brain, whereas the anti-*G*1 antibody recognized a 16-kDa band in all tissues (brain and kidney are shown in Fig. 4*A*). The molecular sizes of both bands appeared to be slightly larger than those predicted from the corresponding cDNAs (13.7 and 13.6 kDa, respectively), possibly due to their amino-terminal regions being rich in lysine and arginine.

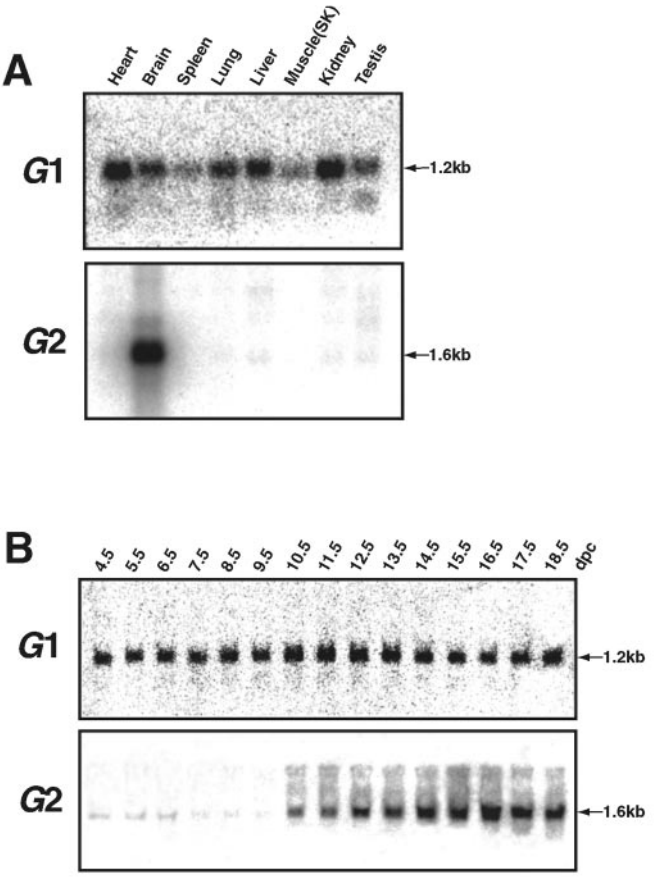

FIG. 2. **Northern blot analysis of *G*1 and *G*2 transcripts in mouse tissues.** Mouse multiple-tissue Northern blots (CLONTECH; 2 μg of poly(A)$^+$ RNA/lane) (*A*) and embryonic stage Northern blots (Seegene) (*B*) were hybridized with the ^{32}P-labeled *G*1 or *G*2 probe. The positions of the *G*1 (1.2 kb) and *G*2 (1.6 kb) transcripts are indicated (*arrows*). *SK*, skeletal; *dpc*, days postcoitus.

G1 and G2 Are Functional V-ATPase Subunits—Membranes were obtained from brains and treated with octyl glucoside. The solubilized V-ATPase fraction was incubated with anti-*G*1 or anti-*G*2 IgG antibody, and the immunoprecipitate was subjected to PAGE. The precipitate contained the *A* and *c* subunits of the V_1 and V_0 sectors, respectively, suggesting that both *G*1 and *G*2 are functional subunits of V-ATPase (Fig. 4*B*).

We have also examined whether or not the mouse isoforms can complement the yeast Δ*vma10* mutant lacking the *G* subunit. The open reading frame of *G*1 or *G*2 was placed under the control of the yeast *TDH3* constitutive promoter, and the resulting plasmid expressing the native *G*1 or *G*2 subunit with or without a Myc tag was introduced into Δ*vma10* cells. The mutant cells could not grow in neutral pH medium (Fig. 5,

[2] Available at gsc.riken.go.jp/e/FANTOM/map/mouse/.

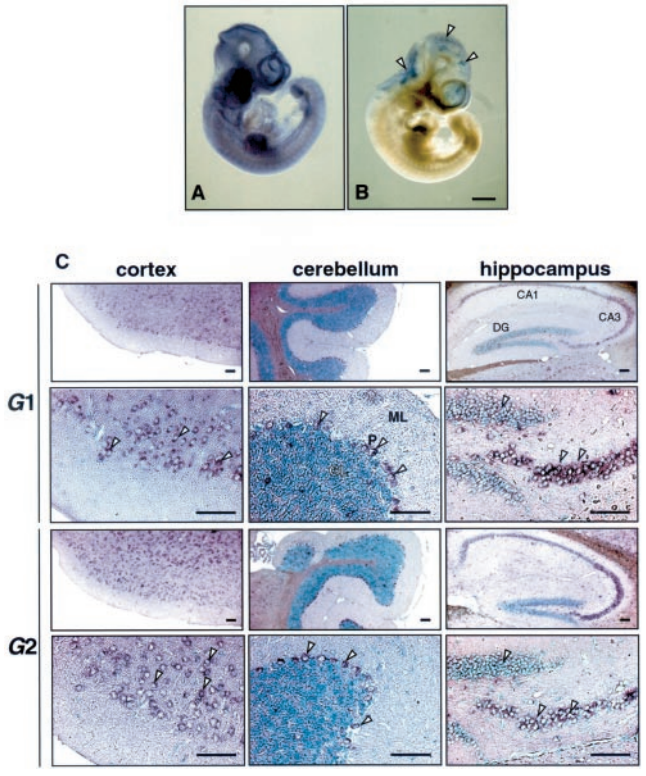

FIG. 3. **Expression of *G*1 and *G*2 transcripts in embryonic and adult mice.** Embryos (10.5 days postcoitus) were hybridized with the *G*1 (*A*) and *G*2 (*B*) probes. The *G*2 expression in the central nervous system is shown (*B*, *arrowheads*). Sections of adult brains were also hybridized with the *G*1 or *G*2 probe (*C*). The cortical, cerebellar, and hippocampal regions are shown. *ML*, molecular layer; *P*, Purkinje cells; *GL*, granular layer; *CA*, Cornu Ammon; *DG*, dentate gyrus. *Scale bars* = 400 μm (*A* and *B*) and 50 μm (*C*).

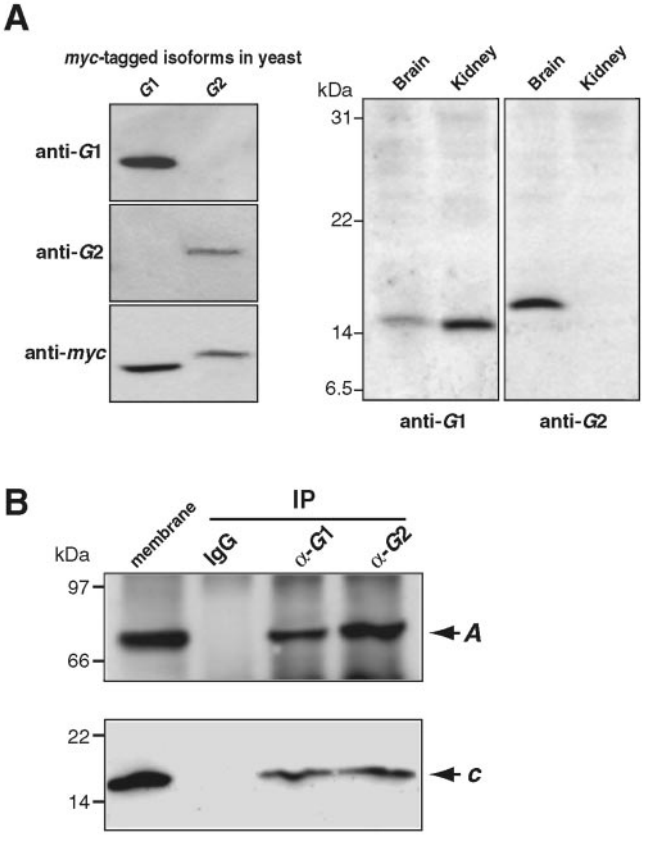

FIG. 4. **Western blot analysis of *G*1 and *G*2 expression and association of the isoforms with other V-ATPase subunits.** *A*, total lysates of murine brain and kidney together with ones of yeast expressing the *G*1-Myc or *G*2-Myc fusion protein were subjected to gel electrophoresis in the presence of SDS. The results from immunoblotting with the purified IgG against each isoform are shown. *B*, the octyl glucoside-solubilized fraction (0.45 mg of protein) was incubated with anti-*G*1 (α-*G1*) or anti-*G*2 (α-*G2*) antibody or control IgG in the buffer used for the solubilization of V-ATPase. Immunoprecipitates (*IP*) were subjected to gel electrophoresis, blotted onto nitrocellulose sheets, and incubated with antibody against the *A* or *c* subunit. The positions of the *A* and *c* subunits are indicated by *arrows*. As a control, the brain membrane fraction was also subjected to electrophoresis (*membrane*).

Vector), whereas those with *VMA10* or mouse *G*2 (without a tag) could (Fig. 5, *VMA10* and *G*2). This indicated that expression of mouse *G*2 functionally complemented Δ*vma10*. Similar complementation was not observed with *G*1 (Fig. 5, *G*1).

Localization of G1 and G2 in Brain—The brain-specific expression of *G*2 suggests that a V-ATPase of this isoform may be involved in neuron-specific function(s). Because both *G*1 and *G*2 are highly expressed in the adult brain, we suspected that the intracellular localizations of the two isoforms may be different. As expected, immunostaining with isoform-specific antibodies revealed that the intracellular localizations of *G*1 and *G*2 were remarkably distinct (Fig. 6). Strong signals for *G*1 were detected in the cell bodies of hippocampal neurons, Purkinje cells, and cerebral neurons, whereas ones for *G*2 were detected in fibers in the axonal region (Fig. 6, *arrowheads*), in addition to cell bodies and dendrites (Fig. 6).

We have labeled *G*1 or *G*2 in cultured hippocampal or cerebellar cells together with brain MAP2 (44), glial fibrillary acidic protein (45), and 2′,3′-cyclic nucleotide 3′-phosphodiesterase (46), markers of neurons, astrocytes, and oligodendrocytes, respectively. *G*1 was positive in the three cell types (Fig. 7, *A–C*), whereas *G*2 was expressed only in MAP2-positive cells (Fig. 7*C*). These results indicated that *G*2 was expressed exclusively in neuronal cells. On the other hand, the ubiquitously distributed *G*1 subunit was expressed in astrocytes and oligodendrocytes, in addition to neurons.

*G*2 was clearly found in the axonal domain in addition to dendrites and cell bodies (Fig. 7*C*). Furthermore, *G*2 staining coincided with staining of synaptophysin (Fig. 8), a protein marker of synaptic vesicles (47). In contrast, *G*1 was expressed in cell bodies and somatodendritic compartments, but no specific staining was detected in the axonal regions (Fig. 7*C*, *arrowheads*). We have also examined the localization of *G*1 and *G*2 in axonal regions using immunoelectron microscopy. *G*2 was detected in presynaptic vesicles (Fig. 8*D*, *arrows*), whereas no *G*1 was found in these regions (Fig. 8*E*). The subcellular distribution of the *G*2 subunit was similar to that of the *A* or *c* subunit of V-ATPase during brain fractionation, and these subunits were enriched in the synaptic vesicle preparation (Fig. 9*A*, *SV*). In contrast, *G*1 was not detectable in synaptosomal fractions and purified synaptic vesicles, although it could be detected in other fractions with V-ATPase subunits. Taken together, these results suggest that synaptic vesicles contain a unique V-ATPase with the *G*2 isoform, but not ubiquitous *G*1 subunit. The *G*2 isoform and the *A* subunit were also found in the soluble fraction (LS2), which contained a significantly reduced amount of synaptophysin and the *c* subunit (Fig. 9*A*). This result is consistent with previous findings (48, 49), suggesting a dynamic association-dissociation between the cytosolic and transmembrane portions of the V-ATPase.

Enzymatic Properties of V-ATPase with the G1 or G2 Isoform—It was of interest to compare the enzymatic properties of

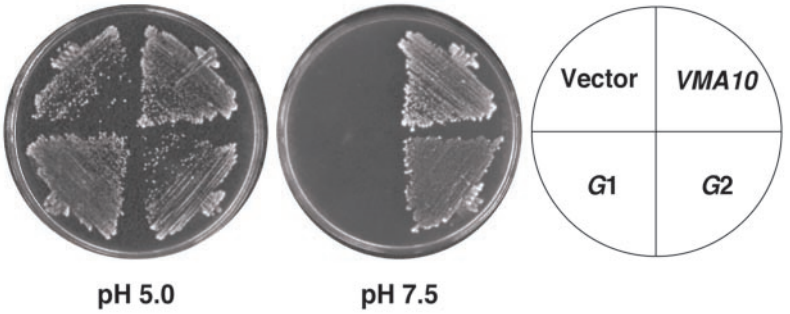

FIG. 5. **Functional complementation of the yeast Δ*vma10* mutation by mouse *G2*.** The yeast mutant Δ*vma10* harboring the vector (*Vector*) or the expression plasmid for *G*1, *G*2, or *VMA10* was streaked onto YPD (yeast/peptone/dextrose) plates buffered at pH 5.0 or 7.5 and then incubated for 4 days at 30 °C.

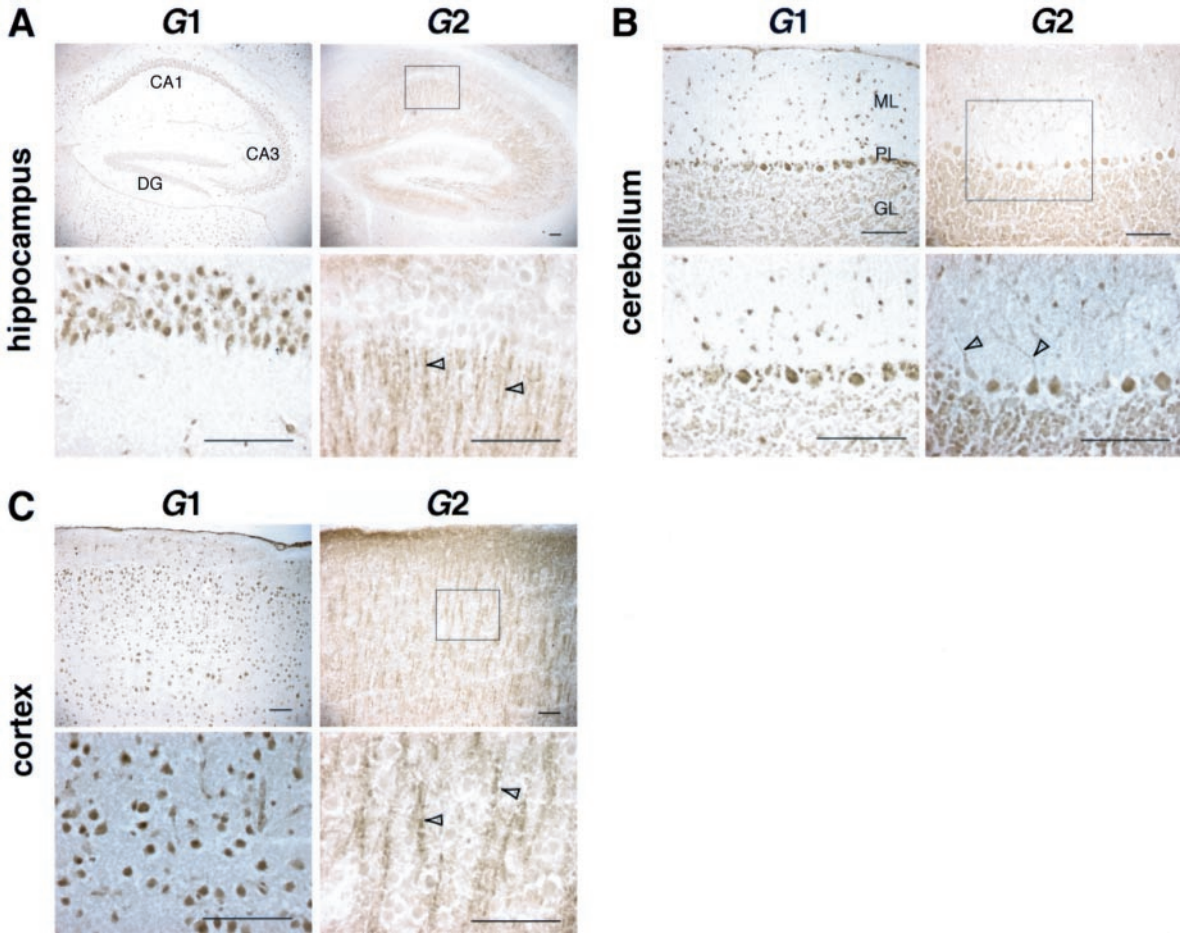

FIG. 6. **Localization of the *G*1 and *G*2 proteins in brain.** Sections of mouse brains were stained with antibodies against *G*1 and *G*2. The hippocampal (*A*), cerebellar (*B*), and cortical (*C*) regions are shown. The *boxed* areas are shown at greater magnification in the *lower panels*. The localization of *G*2 in fibrous structures is indicated by *arrowheads*. *CA*, Cornu Ammon; *DG*, dentate gyrus; *ML*, molecular layer; *PL*, Purkinje cell layer; *GL*, granular layer. *Scale bars* = 50 μm.

the pumps containing the *G*1 and *G*2 isoforms, respectively. We measured the $K_{m(ATP)}$ and V_{max} for concanamycin A-sensitive ATP hydrolysis using the purified synaptic vesicles containing V-ATPase with *G*2 and lysosomal membranes containing only *G*1 (Fig. 9*B*, *fr. 17*). The $K_{m(ATP)}$ was 252 μM for synaptic vesicles (*G*2) and 250 μM for lysosomal membranes (*G*1) (Table I), indicating that the *G*1- and *G*2-containing enzymes have no kinetic difference. It was also of interest to determine whether the kinetic property of V-ATPase with *G*1 or *G*2 was retained with the purified enzyme. The anti-*G*1 or *G*2 antibody (added at a 1:1 protein ratio of antibodies to vesicles) had no effect on ATP-dependent proton transport in synaptic vesicles or lysosomal vesicles, indicating that the antibodies could be used for immunoaffinity purification. The V-ATPase with *G*1 or *G*2 bound to the affinity beads retained concanamycin A-sensitive ATPase activity. The $K_{m(ATP)}$ value for *G*1 or *G*2 was comparable to that observed with the enzyme in the organellar membranes (Table I).

DISCUSSION

Essential steps for neural chemical transmission include the accumulation of neurotransmitters in synaptic vesicles and their release through regulated exocytosis. For the concentration of neurotransmitters, specific vesicular transporters couple with the electrochemical proton gradient generated by V-ATPase (6, 7, 9–11). Thus, V-ATPases play key physiological roles in the nervous system. One important question to be answered is how the V-ATPases localized in synaptic vesicles reach the axon terminals. There is evidence suggesting that synaptic vesicles are assembled at the axon terminals and that

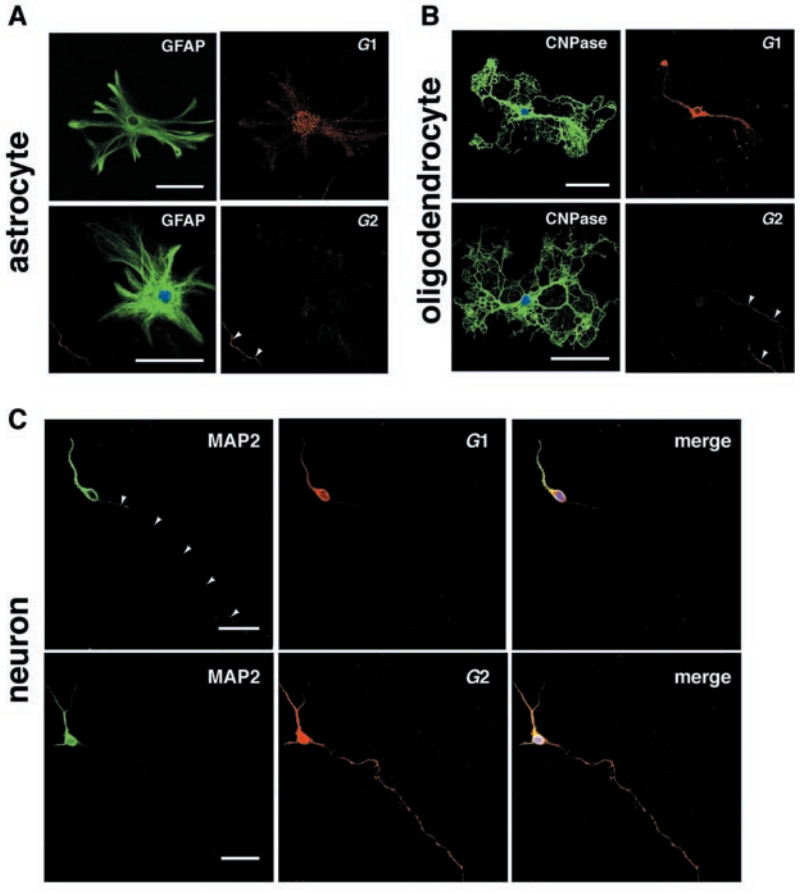

FIG. 7. **Subcellular localization of *G*1 and *G*2 in hippocampal primary cell cultures.** Cells were double-stained with antibody against *G1* or *G*2 and markers for astrocytes (glial fibrillary acidic protein (*GFAP*)) (*A*), oligodendrocytes (2′,3′-cyclic nucleotide 3′-phosphodiesterase (*CNPase*)) (*B*), and neurons (MAP2) (*C*). *G*1 was positive in the three cell types (*A–C*), whereas *G*2 was expressed only in MAP2-positive cells (*C*). *Arrowheads* indicate the axonal regions. The axonal staining of *G*2 in neighboring neurons in *A* and *B* is also indicated (*arrowheads*). Merged images of *G*1 and *G*2 with MAP2, respectively, are also shown in *C*. *Scale bars* = 50 μm.

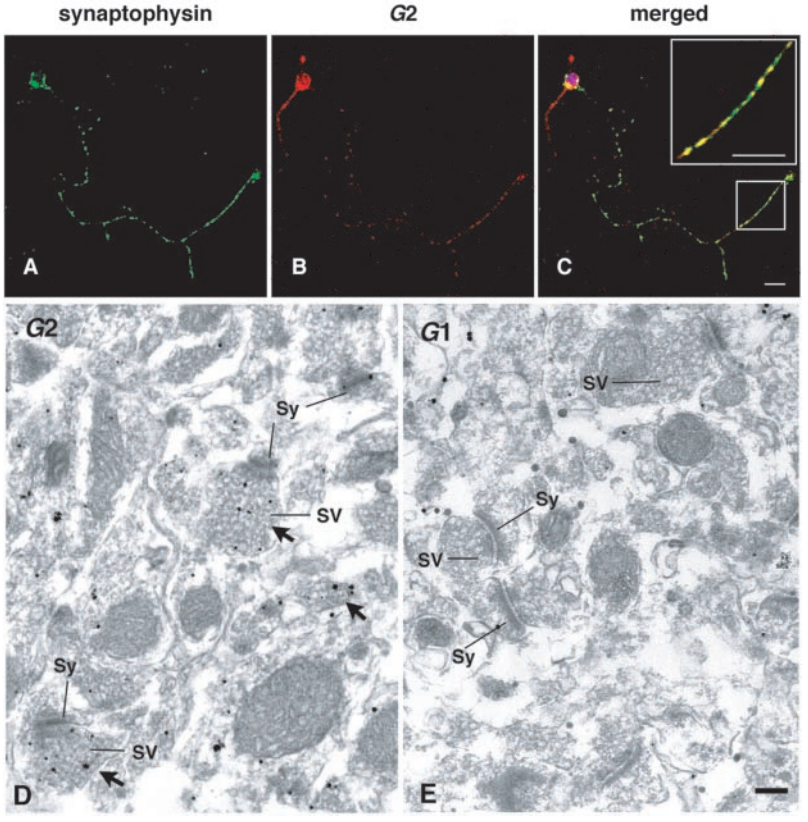

FIG. 8. **Co-localization of *G*2 with synaptophysin.** Hippocampal neurons cultured for 14 days were stained with anti-synaptophysin antibody (*A*) and anti-*G*2 IgG (*B*). A merged image is also shown (*C*), and the *boxed* region is magnified. *Scale bar* = 15 μm. Electron microscopic localization of the *G*2 isoform in presynaptic vesicles is also shown by electron-dense silver-enhanced immunogold particles (*D*, see *arrows* for examples). *G*1 signals were not found in the presynaptic vesicle region (*E*). *Sy*, synapse; *SV*, presynaptic vesicles. *Scale bar* = 500 nm.

their proteins are carried to endosomes and the plasmalemma of nerve terminals in precursor membranes (for a review, see Ref. 50). It is not known whether or not fully functional V-ATPases are transported to the axonal terminals. In this regard, Morel *et al.* (51) observed that the *B* and *c* subunits exhibit different transport rates in *Torpedo* axons. Their re-

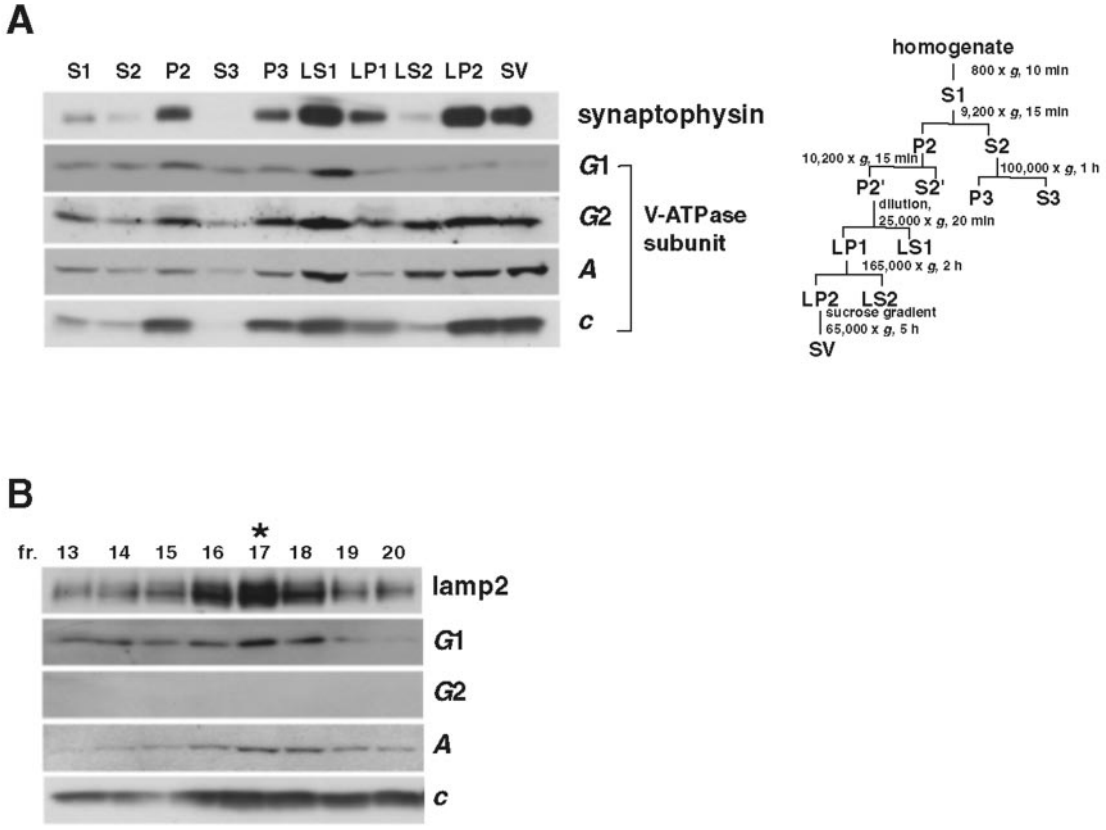

FIG. 9. **Preparation of synaptic vesicles and lysosomal membranes containing different V-ATPases with the *G*1 or *G*2 isoform.** *A*, presence of V-ATPase in brain subcellular fractions. Brain homogenate was fractionated (*right*), and each fraction was subjected to Western blotting (*left*). *SV*, synaptic vesicle fractions. LP2 is the crude synaptic vesicle fraction before gradient centrifugation, and LS2 is synaptosomal fraction. The amounts of fractions subjected to gel electrophoresis were as follows: synaptic vesicles, 5 μg of protein; and other fractions, 20 μg of protein. *B*, preparation of lysosomes with V-ATPase containing the *G*1 isoform. Lysosomal membranes were prepared by OptiPrep density gradient centrifugation (10–35% iodixanol; total volume of 12.5 ml) and fractionated into 25 tubes (0.5 ml/tube, numbered from the bottom). Fractions (10 μl; *fr.*) were subjected to gel electrophoresis, followed by Western blotting with antibodies against LAMP-2 and the *G*1, *G*2, *A*, and *c* subunits. The *asterisk* indicates the fraction used in the measurement of ATPase activity (Table I).

TABLE I
Kinetic analysis of V-ATPase containing G1 or G2

V-ATPase with *G* subunit isoform	ATPase activity[a]	
	$K_{m(ATP)}$	V_{max}
	μM	*nmol/min/mg*
*G*2, synaptic vesicles	252	37.0
*G*1, liver lysosomal vesicles	250	40.6
*G*2, brain, immunopurified	286	70
*G*1, brain, immunopurified	223	60

[a] ATPase activities were measured in purified synaptic vesicles containing *G*2 (8 μg of membrane protein) or in liver lysosomal membranes containing *G*1 (30 μg of membrane protein), or immunopurified enzyme (0.1 μg). Activities were measured with or without 1 μM concanamycin A, and the results shown represent the concanamycin A-sensitive fraction of the activity. K_m and V_{max} were calculated from Lineweaver-Burk plots of the reciprocal of the initial ATP concentration *versus* the reciprocal of the initial rate of ATPase activity (nmol/min/mg).

sults suggest that the V_1 and V_0 domains are transported separately in axons. It is also of interest to know whether neurons or synaptic vesicles have a unique V-ATPase.

We have identified two isoforms (*G*1 and *G*2) of the mouse V_1 *G* subunit. Immunoprecipitation demonstrated that both isoforms were associated with other V-ATPase subunits. In addition, the *G*2 (but not the *G*1) isoform functionally complemented the yeast counterpart *VMA10* null mutation, indicating that mouse *G*2 can assemble with other V-ATPase subunits to form a functional enzyme complex. On the other hand, yeast V-ATPase with mouse *G*1 was not functional. The defect of the enzyme may be due to the weakly conserved carboxyl-terminal region, which may be required for the assembly of the *G* subunit with V-ATPase.

Interestingly, *G*2 was expressed specifically in brain and was localized exclusively in neurons. Immunofluorescence microscopy, immunoelectron microscopy, and subcellular fractionation revealed that a V-ATPase with *G*2 was localized in synaptic vesicles. In contrast, ubiquitous *G*1 was localized mainly in cell bodies and the proximal portions of dendrites, but was not detectable in axons, as shown by immunofluorescence microscopy and confirmed with immunogold staining by electron microscopy. It is possible that the V-ATPases with *G*1 and *G*2 may differ in their activities. However, we found that the synaptic vesicle V-ATPase with *G*2 and the lysosomal membrane V-ATPase with *G*1 showed similar kinetic properties. Essentially the same kinetic results were obtained with immunopurified V-ATPase (*G*1 or *G*2). Thus, it became of interest to examine whether the *G* subunit isoforms are involved in the transport of V-ATPases to specific destinations because only those with *G*2 were targeted to the synaptic vesicles.

Two bovine *G* isoforms have been purified previously (27). They showed differential expressions in tissues: *G*1, brain, kidney, heart, and spleen; and *G*2, brain. Recombinant bovine *G*1 and *G*2 exhibited different Ca^{2+}- and Mg^{2+}-activated ATPase activities when reconstituted with the *A*, *B*, *C*, and *E* subunits (27). However, the two isoforms were isolated by different procedures, suggesting that their observation could not due to the intrinsic properties of V-ATPase with *G*1 or *G*2 because purification procedures for recombinant isoforms may

affect reconstitution. In this regard, we found that the V-ATPases with *G*1 from lysosomal membranes and with *G*2 from synaptic vesicles, respectively, showed similar ATPase activities.

The human and mouse *G*2 isoforms were mapped adjacent to the major histocompatibility complex class III locus (52). Many genes in the class III region of the human major histocompatibility complex encode proteins involved in immune and inflammatory responses. A role in the immune responses has been suggested for V-ATPase (53, 54), and interleukin-1 has been shown to modulate its activity in a dose-dependent manner (53). However, we did not detect *G*2 expression in macrophage cell lines (data not shown).

In summary, we have shown that V-ATPase with the *G*2 isoform is specifically localized in neural synaptic vesicles, whereas that with the *G*1 isoform is expressed ubiquitously. The *G*2 isoform may be involved not only in the acidification of synaptic vesicles, but also in the assembly of a functional proton pump to neuron-specific organelles.

Acknowledgments—We are grateful to Akinori Fukuyama for expert technical assistance in the histochemistry experiments. We are also grateful to Sachiko Shimamura and Mikako Nakashima for preparation of the manuscript.

REFERENCES

1. Nelson, N., and Harvey, W. R. (1999) *Physiol. Rev.* **79,** 361–385
2. Stevens, T. H., and Forgac, M. (1997) *Annu. Rev. Cell Dev. Biol.* **13,** 779–808
3. Futai, M., Oka, T., Sun-Wada, G.-H., Moriyama, Y., Kanazawa, H., and Wada, Y. (2000) *J. Exp. Biol.* **203,** 107–116
4. Wieczorek, H., Brown, D., Grinstein, S., Ehrenfeld, J., and Harvey, W. R. (1999) *Bioessays* **21,** 637–648
5. Gluck, S. L., Underhill, D. M., Iyori, M., Holliday, I. S., Kostrominova, T. Y., and Lee, B. S. (1996) *Annu. Rev. Physiol.* **58,** 427–445
6. Füldner, H. H., and Stadler, H. (1982) *Eur. J. Biochem.* **121,** 519–524
7. Michaelson, D. M., and Angel, I. (1980) *Life Sci.* **27,** 39–44
8. Stadler, H., and Tsukita, S. (1984) *EMBO J.* **3,** 3333–3337
9. Moriyama, Y., Maeda, M., and Futai, M. (1992) *J. Exp. Biol.* **172,** 171–178
10. Moriyama, Y., and Futai, M. (1990) *Biochem. Biophys. Res. Commun.* **17 3,** 443–448
11. Moriyama, Y., Tsai, H. L., and Futai, M. (1993) *Arch. Biochem. Biophys.* **305,** 278–281
12. Hanada, H., Hasebe, M., Moriyama, Y., Maeda, M., and Futai, M. (1991) *Biochem. Biophys. Res. Commun.* **176,** 1062–1067
13. Hayami, K., Noumi, T., Inoue, H., Sun-Wada, G.-H., Yoshimizu, T., and Kanazawa, H. (2001) *Gene* (*Amst.*) **273,** 199–206
14. Sun-Wada, G.-H., Murata, Y., Yamamoto, A., Kanazawa, H., Wada, Y., and Futai, M. (2000) *Dev. Biol.* **228,** 315–325
15. Inoue, H., Noumi, T., Nagata, M., Murakami, H., and Kanazawa, H. (1999) *Biochim. Biophys. Acta* **1413,** 130–138
16. Oka, T., Toyomura, T., Honjo, K., Wada, Y., and Futai, M. (2001) *J. Biol. Chem.* **276,** 33079–33085
17. Mattsson, J. P., Li, X., Peng, S. B., Nilsson, F., Andersen, P., Lundberg, L. G., Stone, D. K., and Keeling, D. J. (2000) *Eur. J. Biochem.* **267,** 4115–4126
18. Toyomura, T., Oka, T., Yamaguchi, C., Wada, Y., and Futai, M. (2000) *J. Biol. Chem.* **275,** 8760–8765
19. Nishi, T., and Forgac, M. (2000) *J. Biol. Chem.* **275,** 6824–6830
20. Oka, T., Murata, Y., Namba, M., Yoshimizu, T., Toyomura, T., Yamamoto, A., Sun-Wada, G.-H., Hamasaki, N., Wada, Y., and Futai, M. (2001) *J. Biol. Chem.* **276,** 40050–40054
21. Smith, A. N., Finberg, K. E., Wagner, C. A., Lifton, R. P., Devonald, M. A., Su, Y., and Karet, F. E. (2001) *J. Biol. Chem.* **276,** 42382–42388
22. Peng, S. B., Li, X., Crider, B. P., Zhou, Z., Andersen, P., Tsai, S. J., Xie, X. S., and Stone, D. K. (1999) *J. Biol. Chem.* **274,** 2549–2555
23. Smith, A. N., Skaug, J., Choate, K. A., Nayir, A., Bakkaloglu, A., Ozen, S., Hulton, S. A., Sanjad, S. A., Al-Sabban, E. A., Lifton, R. P., Scherer, S. W., and Karet, F. E. (2000) *Nat. Genet.* **26,** 71–75
24. Li, Y.-P., Chen, W., Liang, Y., Li, E., and Stashenko, P. (1999) *Nat. Genet.* **23,** 447–451
25. Karet, F. E., Finberg, K. E., Nelson, R. D., Nayir, A., Mocan, H., Sanjad, S. A., Rodriguez-Soriano, J., Santos, F., Cremers, C. W., Di Pietro, A., Hoffbrand, B. I., Winiarski, J., Bakkaloglu, A., Ozen, S., Dusunsel, R., Goodyer, P., Hulton, S. A., Wu, D. K., Skvorak, A. B., Morton, C. C., Cunningham, M. J., Jha, V., and Lifton, R. P. (1999) *Nat. Genet.* **21,** 84–90
26. Sun-Wada, G.-H., Imai-Senga, Y., Yamamoto, A., Murata, Y., Hirata, T., Wada, Y., and Futai, M. (2002) *J. Biol. Chem.* **277,** 18098–18105
27. Crider, B. P., Andersen, P., White, A. E., Zhou, Z., Li, X., Mattsson, J. P., Lundberg, L., Keeling, D. J., Xie, X. S., Stone, D. K., and Peng, S. B. (1997) *J. Biol. Chem.* **272**, 10721–10728
28. Supekova, L., Supek, F., and Nelson, N. (1995) *J. Biol. Chem.* **270,** 13726–13732
29. Murata, Y., Kodama, H., Abe, T., Ishida, N., Nishimura, M., Levinson, B., and Packman, S. (1997) *Pediatr. Res.* **42,** 436–442
30. Sun-Wada, G.-H., Manabe, S., Yoshimizu, T., Yamaguchi, C., Oka, T., Wada, Y., and Futai, M. (2000) *J. Biochem.* (*Tokyo*) **127,** 703–709
31. Tanaka, K., Nakafuku, M., Tamanoi, F., Kaziro, Y., Matsumoto, K., and Toh-e, A. (1990) *Mol. Cell. Biol.* **10,** 4303–4313
32. Tomashek, J. J., Graham, L. A., Hutchins, M. U., Stevens, T. H., and Klionsky, D. J. (1997) *J. Biol. Chem.* **272,** 26787–26793
33. Yamashiro, C. T., Kane, P. M., Wolczyk, D. F., Preston, R. A., and Stevens, T. H. (1990) *Mol. Cell. Biol.* **10,** 3737–3749
34. Nezu, J., Motojima, K., Tamura, H., and Ohkuma, S. (1992) *J. Biochem.* (*Tokyo*) **112,** 212–219
35. Huttner, W. B., Schiebler, W., Greengard, P., and De Camilli, P. (1983) *J. Cell Biol.* **96,** 1374–1388
36. Graham, J., Ford, T., and Rickwood, D. (1994) *Anal. Biochem.* **220,** 367–373
37. Nakamura, N., Yamamoto, A., Wada, Y., and Futai, M. (2000) *J. Biol. Chem.* **275,** 6523–6529
38. Tanabe, M., Nishio, K., Iko, Y., Sambongi, Y., Iwamoto-Kihara, A., Wada, Y., and Futai, M. (2001) *J. Biol. Chem.* **276,** 15269–15274
39. Gluck, S., and Caldwell, J. (1987) *J. Biol. Chem.* **262,** 15780–15789
40. Brewer, G. J., Torricelli, J. R., Evege, E. K., and Price, P. J. (1993) *J. Neurosci. Res.* **35,** 567–576
41. Laemmli, U. K. (1970) *Nature* **227,** 680–685
42. Carninci, P., Shibata, Y., Hayatsu, N., Sugahara, Y., Shibata, K., Itoh, M., Konno, H., Okazaki, Y., Muramatsu, M., and Hayashizaki, Y. (2000) *Genome Res.* **10,** 1617–1630
43. Nornes, H. O., and Carry, M. (1978) *Brain Res.* **159,** 1–6
44. Huber, G., and Matus, A. (1984) *J. Neurosci.* **4,** 151–160
45. Reeves, S. A., Helman, L. J., Allison, A., and Israel, M. A. (1989) *Proc. Natl. Acad. Sci. U. S. A.* **86,** 5178–5182
46. Reynolds, R., Carey, E. M., and Herschkowitz, N. (1989) *Neuroscience* **28,** 181–188
47. Wiedenmann, B., and Franke, W. W. (1985) *Cell* **41,** 1017–1028
48. Galli, T., McPherson, P. S., and De Camilli, P. (1996) *J. Biol. Chem.* **271,** 2193–2198
49. Myers, M., and Forgac, M. (1993) *J. Cell. Physiol.* **156,** 35–42
50. Hannah, M. J., Schmidt, A. A., and Huttner, W. B. (1999) *Annu. Rev. Cell Dev. Biol.* **15,** 733–798
51. Morel, N., Gérard, V., and Shiff, G. (1998) *J. Neurochem.* **71,** 1702–1708
52. Neville, M. J., and Campbell, R. D. (1999) *J. Immunol.* **162,** 4745–4754
53. Brisseau, G. F., Grinstein, S., Hackam, D. J., Nordström, T., Manolson, M. F., Khine, A. A., and Rotstein, O. D. (1996) *J. Biol. Chem.* **271,** 2005–2011
54. Swallow, C. J., Grinstein, S., Sudsbury, R. A., and Rotstein, O. D. (1990) *Surgery* **108,** 363–368